

## THE IMPACT OF ATMOSPHERIC FORCING AND WATER COLUMN STRATIFICATION ON THE YEARLY PLANKTON CYCLE

J. V. STANEVA<sup>1</sup>, E. V. STANEV<sup>1</sup> and T. OGUZ<sup>2</sup>

<sup>1</sup> *Department of Meteorology and Geophysics,  
University of Sofia, 5, James Bourchier street, 1126 Sofia, Bulgaria*

<sup>2</sup> *Institute of Marine Sciences,  
Middle East Technical University, Erdemli, İçel, Turkey*

### Abstract

Heat, fresh water and momentum fluxes at sea surface, which are based on atmospheric analyses data are used to force coupled physical-biological model of the Black Sea. The high frequency oscillations provided by this forcing are very important for the temporal variability of the depth of mixing layer and the temperature stratification of the upper ocean. Rapid changes of physical environment occur at time scales of days. These time scales are comparable to the characteristic time scales of plankton system and affect primary production. The paper addresses the impact of vertical stratification on the functioning of biological system, described by a simple (five-compartment) pelagic ecosystem model. Simulations with 1-D mixed layer and 3-D circulation models, coupled with the same biological model, are analyzed. It is shown that the topography of the Black Sea pycnocline presents an important physical factor governing the primary production in the biological model.

### 1. Introduction.

The physical, biological and chemical components of the Black Sea ecosystem are governed by the external forcing (fluxes from the atmosphere, rivers and straits), as well as the specific internal dynamics. Changes in the physical/biological structures associated with changes in the forcing functions resulted in dramatic alteration in the ecosystem in the last 30 years. The evolution of the Black Sea ecosystem caused by these changes is however not easily addressed from survey data due to lack of spatial resolution of measurements and their sparsity. Even though modeling studies are still in their early stage of maturity, due to the inaccurate descriptions/parameterizations of the complex ecological chains in the models, they nevertheless complement



observations and enable to understand the processes and interactions between different compartments if the ecosystem. The present study aims to elucidate some aspects of the functioning of a simple ecological model in realistic physical conditions corresponding to the Black Sea.

The Black Sea circulation can be roughly represented as one cyclonic gyre, encompassing the entire basin and quasipermanent anticyclonic eddies in the coastal zone, which undergo pronounced structural and temporal variability (Oguz *et al.*, 1993). Eddies and meanders are of utmost importance for the exchange of water between the coastal and open sea regions and could have crucial biogeochemical implications in regard to onshore-offshore transports of biogenic materials. Their correct representation is therefore important in the coupled physical-biological-chemical models, because significant amount of nutrients, delivered in the coastal areas by rivers are transported by the meandering currents into the basin interior. Vertical exchanges in the upper layer water column of the Black Sea is studied by recent observations (Ozsoy *et al.*, 1993) and numerical simulations (Stanev, 1990; Stanev *et al.*, 1995; Oguz *et al.*, 1996a; Stanev *et al.*, 1997). Though this exchange is very small due to the extremely strong vertical stratification, it affects drastically not only the physical processes, but also chemical and biological systems. As shown by Staneva and Stanev (1997) the diapycnal mixing depends mostly on the characteristics of motion in the horizontal and is better pronounced along isopycnal surfaces. The simulated patterns of the depth of the  $\sigma_t=14.8$  isopycnal surface for four consecutive months (Figure 1) reveal two important characteristics of the circulation: (1) the transitions due to the seasonal variability, and (2) the baroclinic eddies. The depth of the isopycnal surface changes from 30–40 m in the interior Black Sea to about 100 m at the periphery. The frontal slope is larger in winter, in response to increasing intensity of the circulation in this season. Strong meanders are simulated along the southern coast (Figure 1a). This pattern changes considerably within several months and more than 5 anticyclonic eddies are observed between the interior gyre and the coast in spring. The patterns are relatively smoother in summer (Figure 1c) and even much smoother in fall (Figure 1d). The division of the Black Sea into interior cyclonic region and anticyclonic periphery, separated by the meandering front on the continental slope is clearly evident by the recent basinwide hydrographic observations (Oguz *et al.*, 1993). As it will be demonstrated in the paper, this physical background has a strong impact on the spatial variability of the ecological components.

In the present study we aim to illustrate the basic physical and biological dynamics of upper ocean using physical models coupled with a biological model. The physical models include mixed layer dynamics as the most important physical background for ecological system (Staneva *et al.*, 1998), or full set of primitive equations (Stanev *et al.*, 1997). The biological model is based on the ecosystem model similar to the one described by Fasham *et al.* (1990). Its application to the lower trophic Black Sea ecosystem in relation to the first order physical effects within the mixed layer have been recently presented by Oguz *et al.* (1996b) and Çokasar (1997).

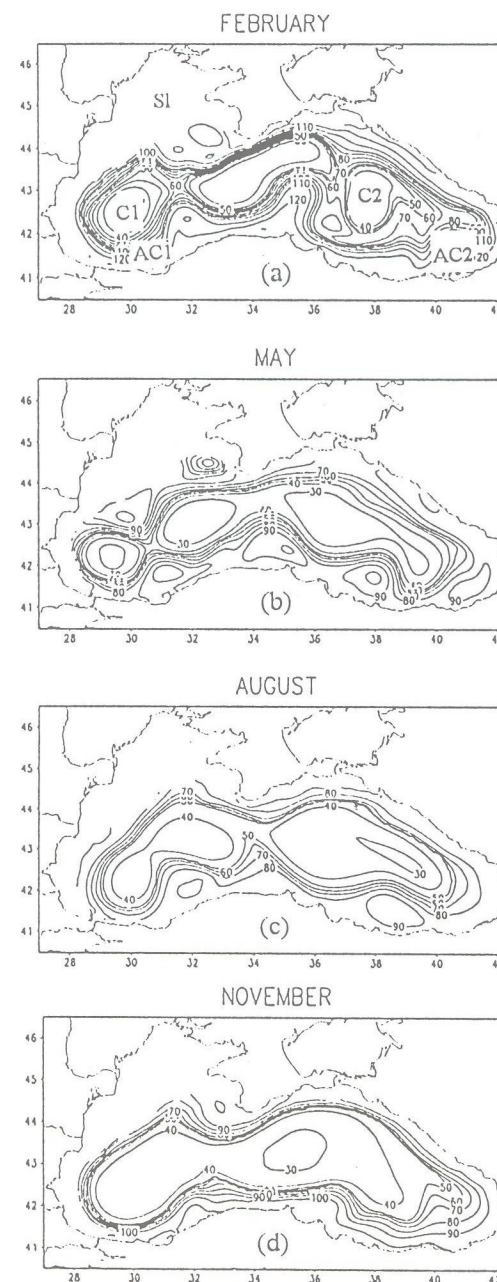


Figure 1. Depths of isopycnal surface  $\sigma_t=14.8$  simulated in the 3-D Black Sea circulation model, described by Staneva and Stanev (1997), Contour Interval (CI) = 10 m. (a) 28 February, 1986; (b) 28 May, 1986; (c) 28 August, 1986; (d) 28 November 1986. Individual locations used further in text are shown by symbols in Figure 1a.



Similar biological model was coupled for the first time with a 3-D primitive equation model of the Black Sea, and the results were reported by Gregoire *et al.* (1997).

The coupled computational system used in the present paper can be regarded as a tool for simulation of annual and interannual upper ocean dynamics and biogenic element cycle in response to changes in the physical systems. The dependency of mixed layer model response to surface forcing on the different stratification in the Black Sea subregions (Staneva *et al.*, 1998) motivates us to address the spatial dependency of ecological processes in 1-D mixed layer model as an important issue of interest in this paper. This does not aim to neglect the role of advection, but rather gives a first order estimate on the impact of major physical factors on the formation of stratification of the biological variables.

Before studying in detail the impact of physical processes on the biogeochemical cycles in complex 3-D coupled models, we will first address the impact of vertical stratification in different Black Sea regions on the biological model behavior using simplified models, which include mixed layer dynamic. Thus, unlike to some previous studies, the present one aims to answer the question to what extent the stratification affects mixing processes and in particular the behavior of coupled physical-biological model. Estimates on the spatial variability of biological system simulated by 3-D coupled model are also given in the paper.

## 2. Description of the model boundary and initial conditions

### 2.1. MIXED LAYER MODEL

The mixed layer model is based on the formulation of Gill and Turner (1976), relating the changes in the potential energy of a vertical water column to the rate of working of wind at sea surface (Mitchell *et al.*, 1985; Gordon and Bottomley, 1985). Since the model is based on the principles of energy conservation we will define below the heat content of the mixed layer  $H$  (which is of depth  $d$ ) and the potential energy  $P$ :

$$H = \rho_0 C_p \int_0^d T(z) dz \quad \text{and} \quad P = -g \int_0^d \rho(z) z dz \quad (1)$$

In above formulae  $\rho_0$  is constant reference density,  $T$  is the potential temperature and  $C_p$  is the specific heat capacity of sea water at surface,  $\rho(z)$  is the potential density with reference to the surface.

The model relates changes in  $P$  to the rate of working by the momentum. The rate of turbulent energy input at the surface due to wind forcing is

$$W = m_0 \rho_w v_*^3, \quad (2)$$

where  $v_*$  is the ocean friction velocity,  $\rho_w$  is the density of sea water, and  $m_0$  is a scaling factor of the order of unity. This is decayed exponentially with depth to prevent overdeepening of the mixed layer in winter. It is used further to mix the surface heat

input throughout the mixed layer. Convection in the model is partly penetrative with 85% of convectively generated turbulent kinetic energy dissipated within the mixed layer. The penetrative short wave flux is represented by a double exponential decay function (Paulson and Simpson, 1977). The mixed layer model calculates density changes resulting from changed temperature and salinity. This makes possible to estimate the work done to increase its potential energy. The main part of the model realizes the vertical mixing, which can be either due to instability, or to available mechanical energy by wind. The model parameters were chosen such that the ranges of simulated mixed layer depth lie in the ranges given in Oguz *et al.* (1996b, their Figure 4a).

The forcing functions of the mixed layer model are: the penetrative (solar) component of surface flux; the non-penetrative heat flux (this contributes to the heating of the top layer) and the mechanical ("wind mixing") energy, which is available for mixing water in the stable stratified column. We give below a short description of the physical forcing.

### 2.2. BOUNDARY CONDITIONS

The net heat flux at sea surface can be represented as:

$$Q^T = Q_s - Q_u, \quad (3)$$

where  $Q_s$  is the downward flux of solar radiation and  $Q_u$  is the net upward flux of radiation emitted by the sea surface via radiative and evaporative-convective processes. The net upward flux  $Q_u = H_a + LE_a + Q_b$  includes the net flux of long wave radiation loss  $Q_b$ , sensible  $H_a$  and latent  $LE_a$  heat flux ( $L=2.501 \cdot 10^6 \text{ J kg}^{-1}$  is the latent heat of vaporization). For the long wave radiation loss we use the formulae of Berliand and Berliand (1952), modified as in Rosati and Miyakoda (1988), and for the sensible and latent heat flux the following bulk formulae:

$$H_a = \rho_a C_p C_h |W| \times (T_s - T_a), \quad (4)$$

$$E_a = \rho_a C_e |W| \times \left[ e_{sat}(T_s) - r e_{sat}(T_a) \right] \frac{0.622}{p_a}, \quad (5)$$

where:  $T_s$  and  $T_a$  are the SST and the atmospheric temperature at 1000 mbar respectively,  $e_{sat}(T_a)$  is polynomial approximation (Lowe, 1977),  $\rho_a$  is the density of the air,  $p_a$  is the surface air pressure ( $p_a=1013 \text{ mbar}$ ),  $|W|$  is the surface wind magnitude,  $C_p$  is the specific heat capacity ( $C_p=1.005 \times 10^3 \text{ J [kg.K]}^{-1}$ ),  $C_h$ ,  $C_e$  are turbulent exchange coefficients.

Wind stress is parameterized as:

$$(\tau^x, \tau^y) = \rho_a C_d |W| (W_x, W_y) \quad (6)$$



where  $W_x$ ,  $W_y$  are the wind components,  $C_d$  is the drag coefficient. Turbulent exchange and drag coefficients are assumed to be equal and dependent on the stratification in the boundary layer (Hellerman and Rosenstein, 1983, see also Staneva and Stanev, 1998). Momentum and heat fluxes are calculated interactively. The fractional cloud cover is inferred at each model step from the monthly mean data (Sorkina, 1974). The value of  $T_s$  in the parameterizations for the wind stress and for the net upward flux is set to be equal to the current SST, simulated by the mixed layer model.

The atmospheric forcing data are prepared by adding high frequency signal from the twice daily atmospheric analysis data, produced in the US National Meteorological Center (NMC) for the period 1980-1986, to the climatic data of Sorkina (1974). The atmospheric quantities in location AC1 (see Figure 1a) from 1 January, 1980 to 31 December, 1987 illustrate not only synoptic and seasonal cycles but also the interannual variability (Figure 2).

The impact of upper layer physics on the biological systems is addressed in number of studies (Wolf and Woods, 1988; Radach and Moll, 1993). It is found that fifty percent of the variance in the interannual variability of the primary production can be attributed to the spring weather conditions (Goldman *et al.*, 1988). This proves that meteorological factors are of utmost importance for the interannual variability. Another component of atmospheric forcing affecting primary production is the short-period meteorological variability (Radach and Moll, 1993).

The short period oscillations and the seasonal variability dominate the forcing spectrum (Figure 2). The annual course of air temperature shows a summer maximum (25-26 °C) and a winter minimum (-2-0 °C). Interannual variability is illustrated by changing minima and maxima of the seasonal signal in different years (e.g. the strong cooling in winters of 1985 and 1986 and relatively warm summers in 1980 and 1984). The relative humidity and wind magnitude show more irregular behavior than the temperature (Stanev *et al.*, 1995).

### 2.3. BIOLOGICAL MODEL

In the present work we do not address the relevancy of biological models with different levels of complexity to the trophic chain in the Black Sea (this issue is addressed by Van Eeckhout and Lancelot, 1997), but rather analyze the impact of physical processes on a very simple biological system (which does not necessarily incorporate all characteristics of a rather diverse Black Sea ecological system). Hence, we use five-compartment biological model, which is based on the model of Fasham *et al.* (1990). The model has the following biological variables: phytoplankton biomass ( $P$ ), herbivore biomass ( $Z$ ), detritus ( $D$ ), nitrates ( $N$ ) and ammonium ( $A$ ). The main features of the model is described in Oguz *et al.* (1996b), but the present version includes some modifications concerning the food-web functioning and the parameterization of zooplankton grazing and mortality.

In the numerical implementation, the local changes of biological variables are defined as a sum of physical and biological parts:

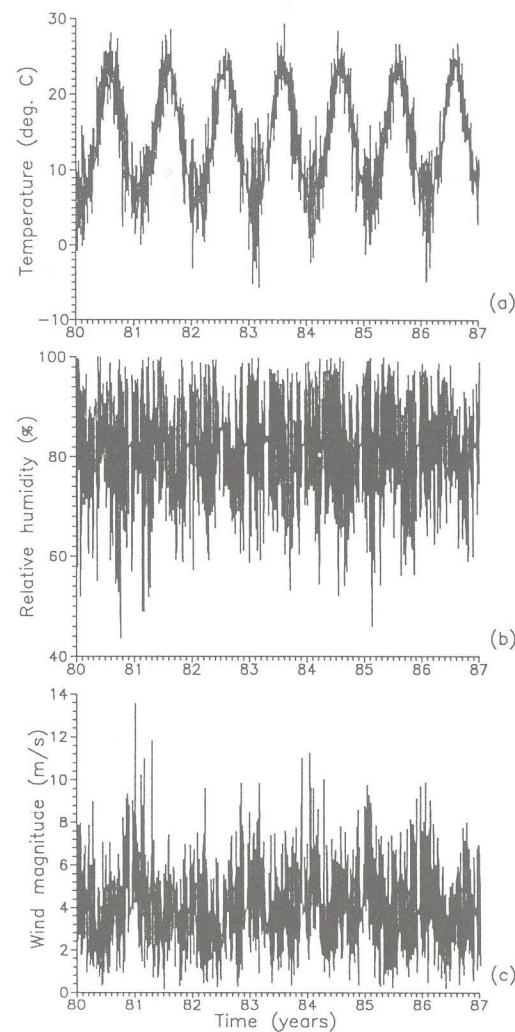


Figure 2. Atmospheric data set in location AC1 for the period from 01 January 1980 to 31 December 1986. (a) air temperature (°C); (b) relative humidity (%); (c) wind magnitude ( $\text{m s}^{-1}$ ).

$$dB/dt = (dB/dt)_{phy} + (dB/dt)_{bio}. \quad (7)$$

For the physical terms we use the same equations, as for temperature and salinity. The term  $(dB/dt)_{phy}$  depends on the complexity of physical model, and includes diffusion, convection and advection (the last when we run 3D simulations). The interactive functions for the biological components and the parameter set are given by Oguz *et al.* (1996b). The rate of change of biomass due to biological processes



$(dB/dt)_{bio}$  is calculated separately from the physical part, thus we split the model into different processes. In the equation of detritus and zooplankton we add additional terms, which describe the grazing of detritus by herbivore (S. Moncheva, personal communication). The boundary and initial conditions in the biological model are as in the study of Oguz *et al.* (1996b): no flux conditions are specified both at the sea surface and at the bottom. The initial profile for nitrates is taken from the same study. The nitrates concentration increases gradually from its surface value (equal to  $0.2 \text{ mmol m}^{-3}$ ) to the subsurface maximum of about  $6 \text{ mmol m}^{-3}$  at 65 m. Close to the oxic/anoxic zone, the concentration of nitrates is less than  $0.1 \text{ mmol m}^{-3}$ . The initial concentrations of other biological compartments are uniform in the whole model column and have the following values: phytoplankton initial concentration- $0.25 \text{ mmol N m}^{-3}$ , herbivore initial concentration- $0.05 \text{ mmol N m}^{-3}$ , detritus initial concentration- $0.05 \text{ mmol N m}^{-3}$ , ammonium initial concentration- $0.05 \text{ mmol N m}^{-3}$ .

The initialization of 1-D mixed layer model and its forcing are formulated in a way to correspond to the major characteristics of the Black Sea subregions with their specific circulation. Thus we extract from the Black Sea GCM simulations (Stanev *et al.*, 1997) annual mean temperature and salinity profiles in different locations, and use them to initialize 1-D model (Figure 3). These locations, are specified such that they correspond to the main peculiarities in the topography of pycnocline: interior cyclonic area (locations C1 and C2), coastal anticyclones (locations AC1 and AC2) and slope area (location SH). We will further analyze the behavior of ecological model in these locations (see Figure 1a).

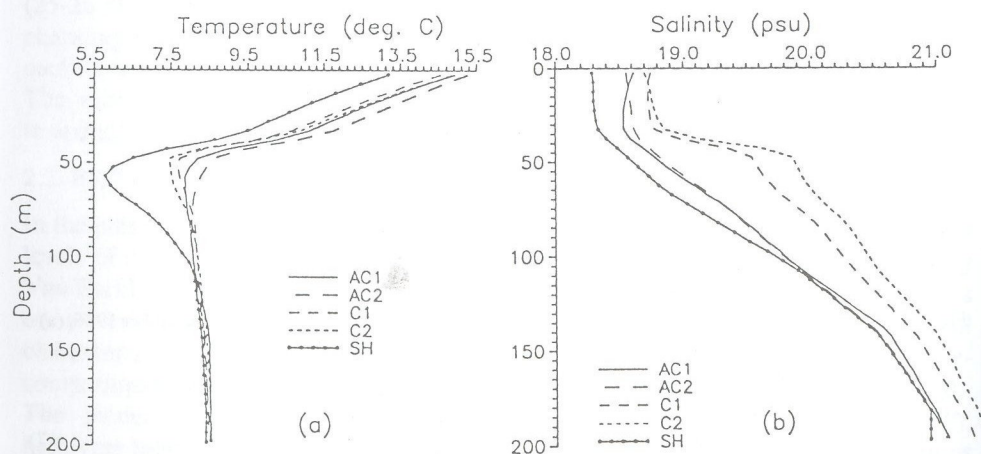


Figure 3. Annual mean temperature and salinity profiles simulated in 3-D OGCM in locations marked in Figure 1a. The specification of different curves is given in legend. (s) temperature [ $^{\circ}\text{C}$ ]; (b) salinity (psu).

The surface waters in the anticyclonic subregion are warmer than in the cyclonic domains. The continental slope (location SH) shows lowest SST compared to the other four sample locations (see asterisk lines in Figure 3). The layer below 120 m is rather homogenous. The upwelling in the basin interior, associated with the cyclonic gyre, explains the shallower position of the halocline than in the coastal areas (Figure 1). As shown by Staneva *et al.* (1998) these peculiarities in stratification affect the depth of mixed layer. This spatial inhomogeneity appears to be an important mechanism governing the nutrient supply from below. Since the stratification is maintained by the seasonal cycle in atmospheric forcing, we anticipate a strong response of ecological model.

### 3. Simulations of the physical characteristic in the different experiments.

The model simulated wind stress magnitude, upward heat flux and solar radiation in location AC1 during the last 3 years of integration are shown in Figure 4. We do not consider the daily cycle, but rather focus on the seasonal and interannual ones, thus the data are presented as daily mean ones. As shown by Staneva *et al.* (1995) and as seen from the present simulations, the variations of atmospheric forcing (Figure 2) have a strong impact on the heat and momentum fluxes at sea surface (Figure 4a, b). The variances in wind stress (more pronounced in winter) are indicative for the magnitude and frequency of occurrence of extreme storms events. The amplitudes of the short-period variability are comparable with those of the seasonal changes. In the cold winters of 1985 and 1986, the heat loss from sea surface exceeds  $1000 \text{ W m}^{-2}$ . These large variances can be reached in only 10 days (see for example falls in 1985 and 1986). Since we do not consider short period and interannual variations for the cloudiness, the short-wave radiation (Figure 4c) repeats periodically.

The variability in the mixed layer depth (MLD) is one of the most important physical quantities governing the coupled physical-biological model. The simulated thickness of mixed layer fluctuates between 5 and 70 m (Figure 5, see also Staneva *et al.*, 1998). Due to the fluctuations in the wind stress and specific surface heating, there are periods (even in winter) when the mixed layer collapses toward sea surface. The largest diurnal oscillations in the MLD occur just prior the spring restratification. In this period the daily average heating is either positive or negative (Figure 4b) and the averaged with a time-window of 10 days heat flux (not shown here) is about zero. At the same time the wind stress magnitude tends to decrease (Figure 4a). The increase in the amplitude of oscillations of MLD in spring was reported earlier by Ozsoy *et al.* (1993) based on survey data and by Staneva *et al.*, 1998) based on model simulations. Similar short periodic variability was simulated by Doney (1996), who used the ECMWF analysis data, Bermuda Atlantic Time Series (BATS) and COADS data to estimate the surface forcing. The forcing obtained from these data was further coupled to 1-D mixed layer model that has much in common with our model setup and resulted in similar estimates about the impact of time variability on the mixed layer dynamics (Staneva *et al.*, 1998).



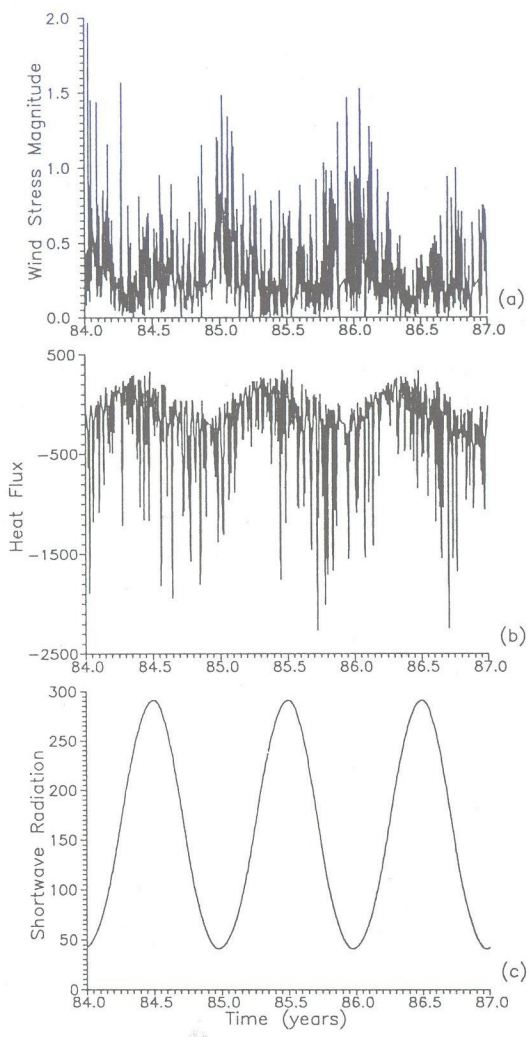


Figure 4. Model simulated data in the last 3 years of integration in location AC1. (a) wind stress magnitude  $\times 10$  [Pa], (b) upward heat flux  $[\text{W m}^{-2}]$ ; (c) solar radiation  $[\text{W m}^{-2}]$ . The abscise axis gives the time (84.0 corresponds to 1 January 1984).

The numerical simulations (Figure 5) give significant interannual variability in the MLD and SST. This is related to the very low atmospheric temperature and strong winds in some years that induce the excess net heat loss of the ocean (note the low SST and the persistent deep convection in winter of 1985-1986). High-frequency variability in the SST (reaching about 0.5-2  $^{\circ}\text{C}$ ) can also be found in the model simulations. These oscillations are better observed in the warm part of the year. However, their amplitude is less pronounced than of the MLD. Below we give a short explanation of this effect. As a result of the strong variations of the MLD, the

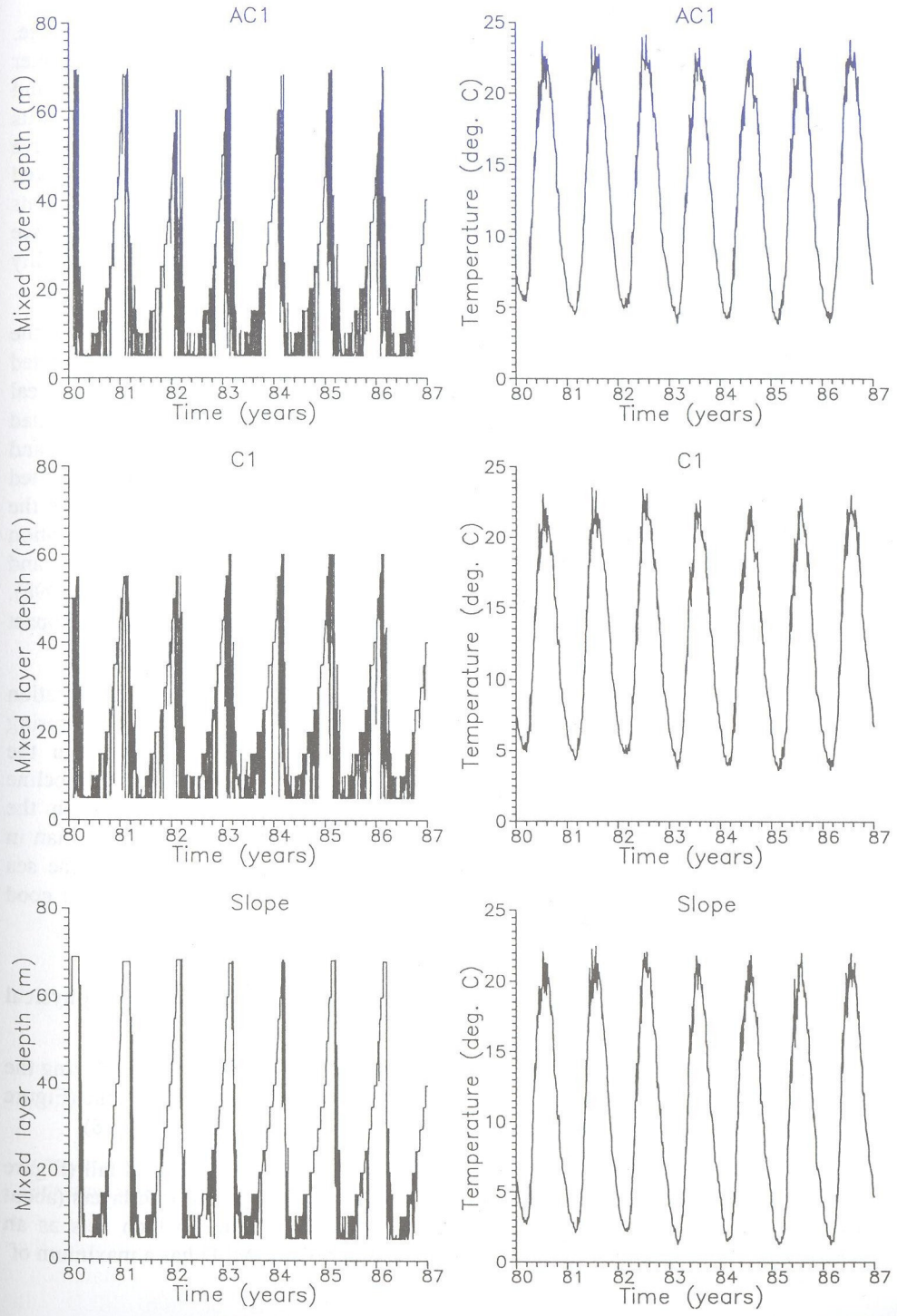


Figure 5. Model simulated mixed layer depth [m], (left column) and SST  $[\text{}^{\circ}\text{C}]$  (right column) for the seven years of integration.



oscillations of SST (particularly in the summer of 1982 and 1983) are relatively large. The in periodic deepening of mixed layer contribute to the entrainment of cold water from below. This maintains larger difference between atmospheric temperature and SST, thus heat fluxes tend to increase. The increase of the thermal stratification, on its side, leads to the shoaling of mixed layer, which is an illustration of the negative feedback mechanism. Therefore, due to the dependency of the forcing on the simulated SST and of the nonlinearity in the bulk parameterization (exchange coefficients depend on the difference between SST and air temperature, and wind magnitude, see Section 2.2), temperature and salinity profiles do not show high frequency variability as pronounced as in the MLD (see Figure 6).

The MLD in the cyclonic locations is about 20-30 m shallower than in the anticyclonic ones (Figure 5). This agrees with the survey data in 1986-1994 reported by Çokasar (1997) and with the model simulations of Staneva *et al.* (1998). In the real sea the large range of variability of MLD is a result of dynamical variability, associated with specific general circulation, as well as with mesoscale features such as eddies and meanders. Similar dependency of MLD and circulation features can not be simulated in 1-D models. To compensate for this drawback of 1-D models we analyze here the simulation results of several sensitivity runs aiming to study the impact of stratification on the ecosystem response. Similar analysis performed in purely physical terms and focused on the water mass formation was done previously by Staneva *et al.* (1998). This simplified approach can be regarded as a first step for understanding the impact of local stratification in ecological models.

The variability of temperature in the upper 70 m for the last 3 years of integration in locations AC1, C1 and SI (see Figure 1) is shown in Figure 6. The time of spring restratification and fall erosion of mixed layer is accurately represented in the evolution of vertical temperature profiles. In fall, the destruction of the thermocline starts one month earlier in 1984 than in the next year. The period when the intermediate water outcrops to the sea surface is twice larger in the slope area than in the central cyclonic and anticyclonic areas. The maximum temperatures at the sea surface are: 25 °C in AC1, 23.7 °C in C1, and 22 °C in the SI, which is in a good consistency with the observed data for the same areas of the Black Sea.

4. Seasonal and interannual biogenic element cycling as a response to physical forcing and vertical stratification.

We will demonstrate here the role of stratification on the annual cycle by analyzing the time evolution of various biological elements integrated over the euphotic zone (Figure 7) as well as of the vertical phytoplankton and zooplankton structure (Figure 8).

The phytoplankton biomass is low (~0.1 mmol N/m<sup>3</sup>) in summer and fall (Figure 7a). This is caused by the reduction of nutrient supply from nutrient rich layers (about 100 m) due to strong stratification in the seasonal thermocline, which acts as an obstacle for the ventilation of deeper levels. In this period the MLD has a maximum of

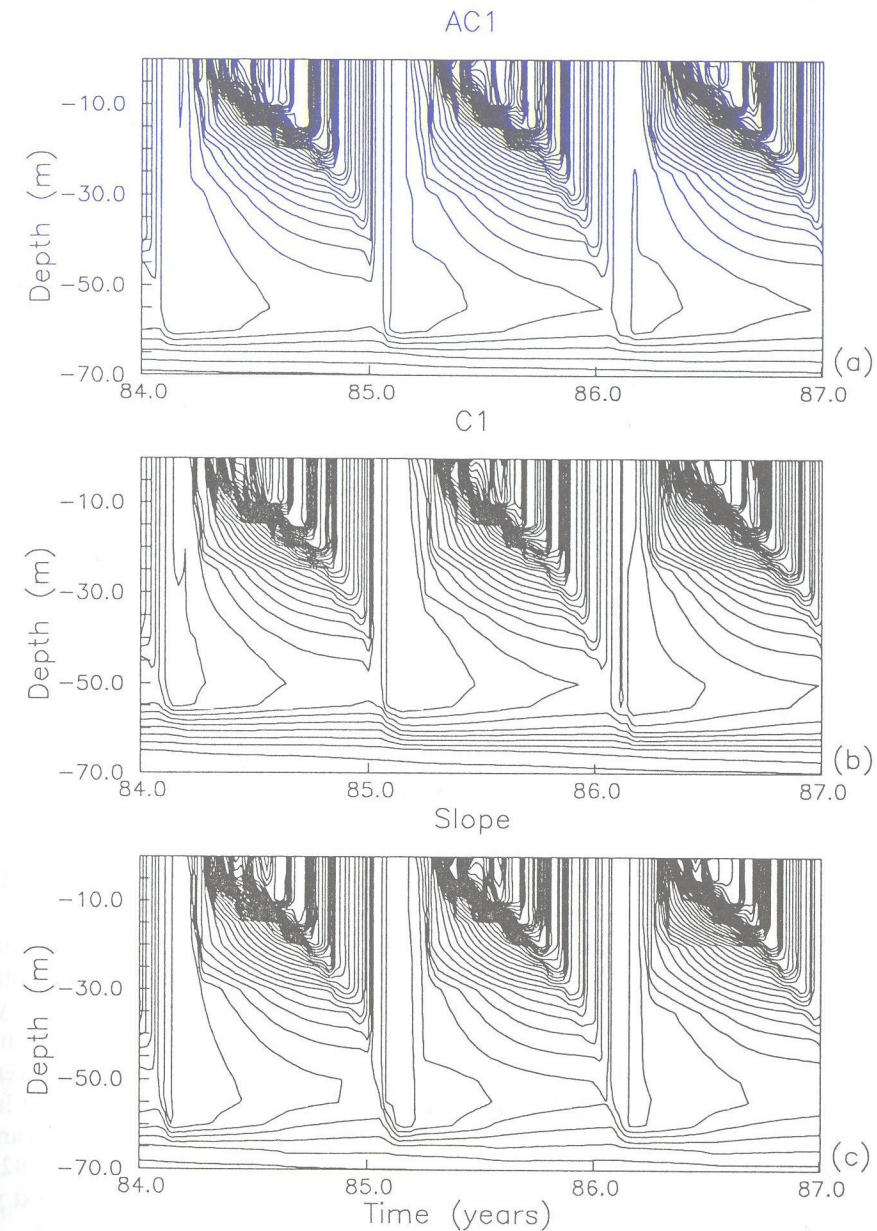


Figure 6. Evolution of the vertical temperature profiles, simulated in one dimensional mixed layer model for locations. (a) AC1 (cmax=25.2 °C, cmin=7.1 °C); (b) C1 (cmax=24.2 °C, cmin=6.7 °C); (c) Slope. CI=0.5 °C (cmax=23.2 °C, cmin=4.6 °C). CI=0.5 °C.



about 20 to 30 m, and the phytoplankton in the euphotic zone is consumed by the zooplankton. The short periodic oscillations of MLD (Figure 5) are about 20 m, and can not reach the layers with larger nutrient concentration. When the mixed layer starts to deepen (in the beginning of October, Figure 5), the surface layer enriches with nutrients (Figure 7e). The fall bloom occurs at the end of November in the areas, dominated by the anticyclonic circulation (Figure 7a). Similar increase of the phytoplankton biomass is not observed in the cyclonic domains, where the increase in the mixed layer is very slow. The bloom thus occurs a month later (in the beginning of the year), when the mixed layer in these locations becomes deep enough. This winter bloom, identified by *Nitzschia delicatula*, was also observed by Mikaelyan (1995) in the central cyclonic gyre.

A month after the fall/winter bloom, the phytoplankton biomass sharply decreases, which is due to the decrease in the nutrient concentration in the upper layer (see the local minimum in the end of 1983 in Figure 7e for the domains with anticyclonic circulation). Another reason for this decrease is the phytoplankton grazing by herbivore. By the end of February, the strong vertical overturning causes a gradual increase of the nitrate concentration (see Figure 7e) that leads to the early spring bloom during the last week of February and the first week of March (in the domains with anticyclonic circulation). For the profile with cyclonic stratification, this occurs by the end of March, with a lower intensity as compared to the first phytoplankton bloom at the beginning of the year. The yearly distributions of herbivore and detritus follow closely that of the phytoplankton with a time lag of 2-4 weeks. The simulations in the anticyclonic areas are quite similar to those of Oguz *et al.* (1996b), therefore we will not discuss below in details the annual behavior of each compartment. From April to August, some local subsurface maxima occur in the phytoplankton production, which are due to the balances between the light and nutrient availability in this period.

The simulated phytoplankton and zooplankton cycles (Figures 8 and 9) undergo variability associated with the interannual variability of the MLD (Figure 5). It is instructive to give some numbers about the amplitudes of interannual oscillations. In 1982 the phytoplankton concentration for AC1 region is  $\sim 1.83 \text{ mmol N/m}^3$ , while in 1985 it is  $\sim 2.34 \text{ mmol N/m}^3$ . The values of the annual maxima in the remaining years of integrations are between these two values:  $\sim 2.15 \text{ mmol N/m}^3$  in 1981,  $\sim 1.97 \text{ mmol N/m}^3$  in 1983,  $\sim 2.21 \text{ mmol N/m}^3$  in 1984 and  $\sim 2.28 \text{ mmol N/m}^3$  in the last year of integration. To better resolve this variability we plotted the figures only for the last 3 years of integration. The time of fall bloom also differs in different years of simulations. It starts by the end of November in 1981 and 1986, whereas in 1982 and 1985 several blooms occur from the end of October to the beginning of the next year. The spring bloom occurs almost at the same time in all years of integration.

The vertical profiles of phytoplankton, simulated in the one-dimensional physical/biological mixed layer model are shown in Figure 10 for the five locations in Figure 1. The curves are plotted for the second week of April, which almost coincides with the time when the maximum of zooplankton biomass is observed (see Figure 9).

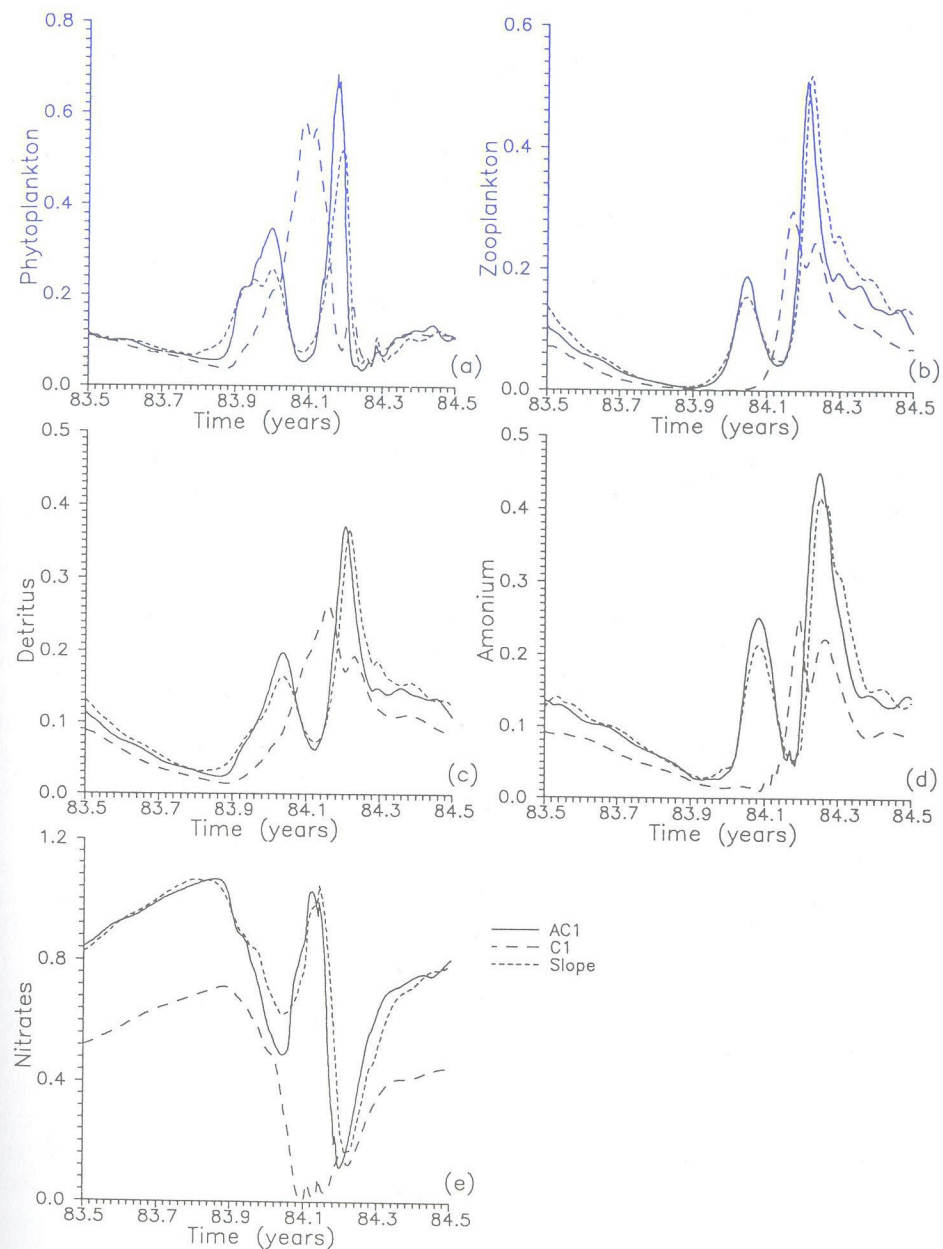


Figure 7. Biogenic elements [ $\text{mmol N m}^{-3}$ ] integrated over the euphotic zone. The curves are shown for one particular year, starting from 1 July 1983.



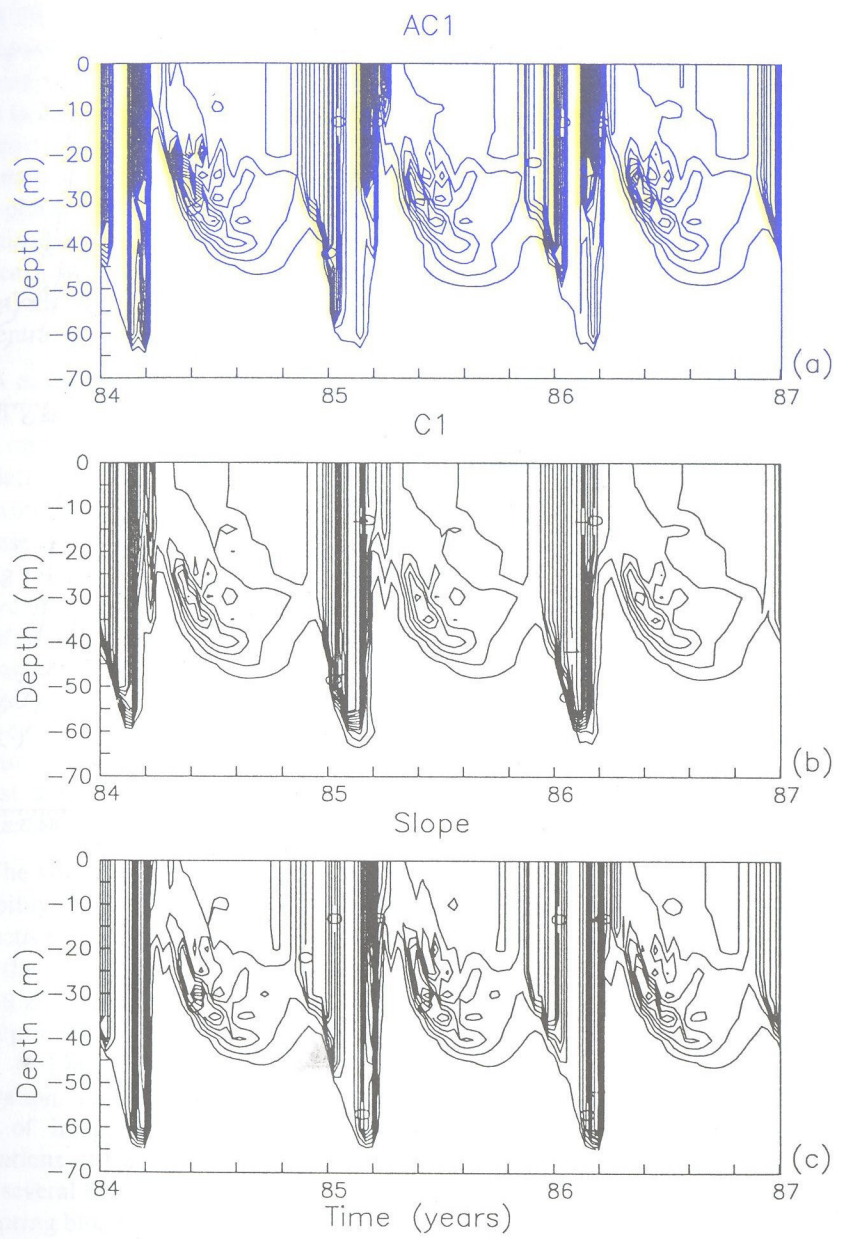


Figure 8. Evolution of the phytoplankton profiles, simulated in one dimensional mixed layer model for locations. (a) AC1 ( $c_{\text{max}}=2.3 \text{ mmol N m}^{-3}$ ); (b) C1 ( $c_{\text{max}}=0.68 \text{ mmol N m}^{-3}$ ); (c) Slope. ( $c_{\text{max}}=0.96 \text{ mmol N m}^{-3}$ ).  $\text{CI}=0.05 \text{ mmol N m}^{-3}$ .

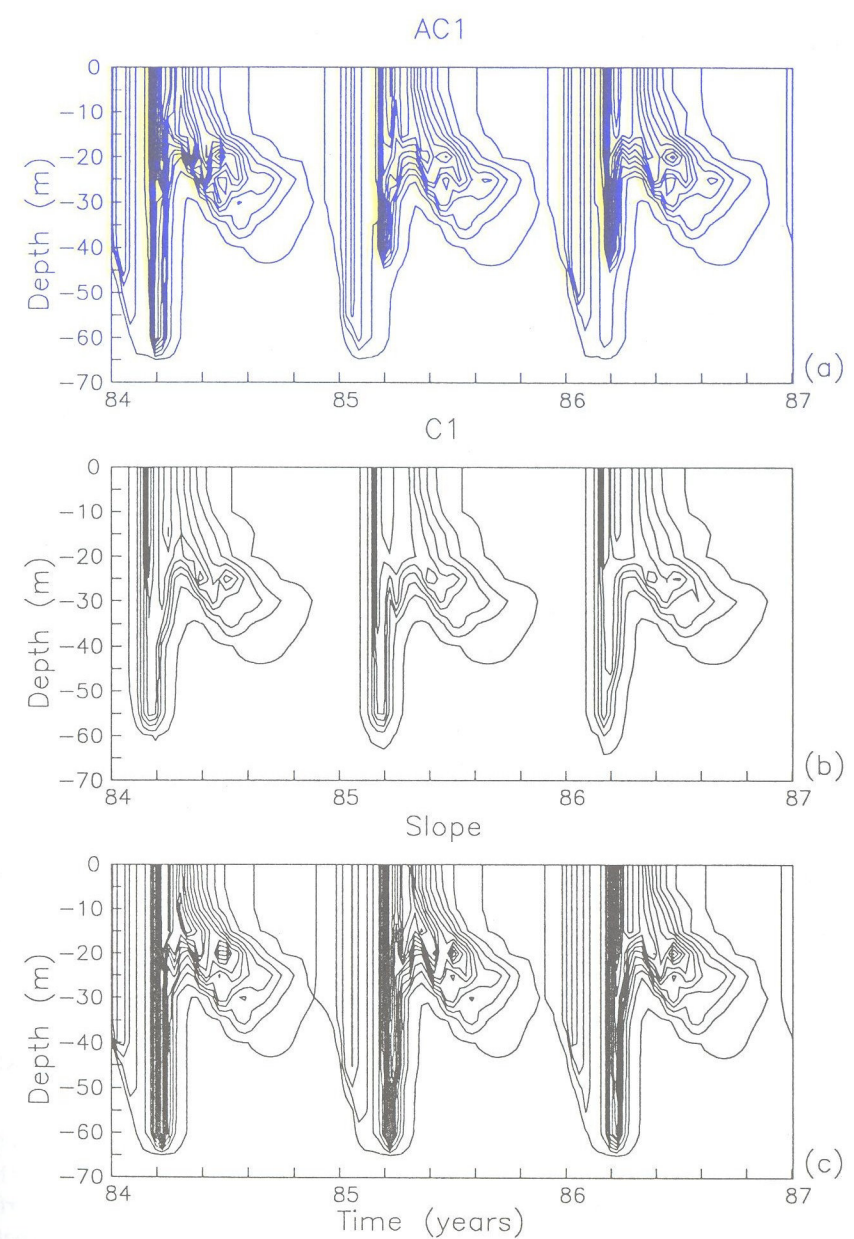


Figure 9. As in Figure 8. But for zooplankton. (a) AC1 ( $c_{\text{max}}=0.71 \text{ mmol N m}^{-3}$ ); (b) C1 ( $c_{\text{max}}=0.53 \text{ mmol N m}^{-3}$ ); (c) Slope ( $c_{\text{max}}=0.73 \text{ mmol N m}^{-3}$ ).  $\text{CI}=0.05 \text{ mmol N m}^{-3}$ .



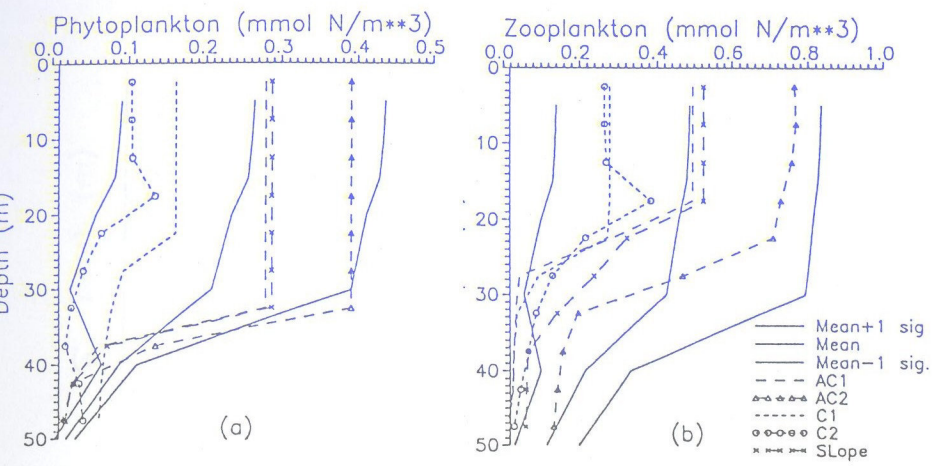


Figure 10. Vertical profiles at 12 April 1986. Simulations from the one dimensional physical/biological mixed layer model in the five sample locations are plotted with dash lines. Area averaged and 1- $\sigma$  deviations from the area averaged simulated in 3-D OGCM are plotted with full lines. (a) phytoplankton; (b) zooplankton.

In the same figure we also show the area averaged concentrations of these biological elements, simulated for the same period in the 3-D OGCM and 1- $\sigma$  deviation in space from the mean value (solid lines). The description of the 3-D physical model, as well as the tracer techniques can be found in the companion paper by Stanev *et al.* (1998, this volume). The initial and boundary conditions and the biology interactive terms, used in 3-D simulations are the same as in the 1-D mixed layer model (see Section 2.3). The results illustrate that the vertical distribution of the phyto- and zooplankton, simulated in the 1-D mixed layer model lies approximately in the range of spatial variability, estimated by the 3-D model. It is noteworthy that the deviations from the mean are of the same order as the mean value. The concentrations in the anticyclonic locations (also in the slope area) are about twice larger than these in the areas dominated by cyclonic circulation. The upper homogeneous layer is about 20 m deeper in the anticyclonic areas than in the cyclonic ones, which correlates with the well known observational evidence. Local subsurface extremums of phytoplankton, supporting the observations, are also simulated (location C2).

We will demonstrate below how important circulation and specific stratification are for the functioning of the model ecosystem by examining the depths of the  $\sigma_t=14.4$  isopycnal surface (Figure 11a), the nitrate distribution along this isopycnal surface (Figure 11b), and along the 17.5 m horizontal surface (Figure 11c). The negative anomalies are plotted with dash lines (mean values are also shown). The depth of the  $\sigma_t=14.4$  isopycnal surface ranges from 65 m in the western basin up to the sea surface in the central part of the sea, where surface outcropping of isopycnal interfaces occurs. The strong variations of the depth of this isopycnal surface in the western area is due to local downwelling-upwelling that occurs at that time of the year. The

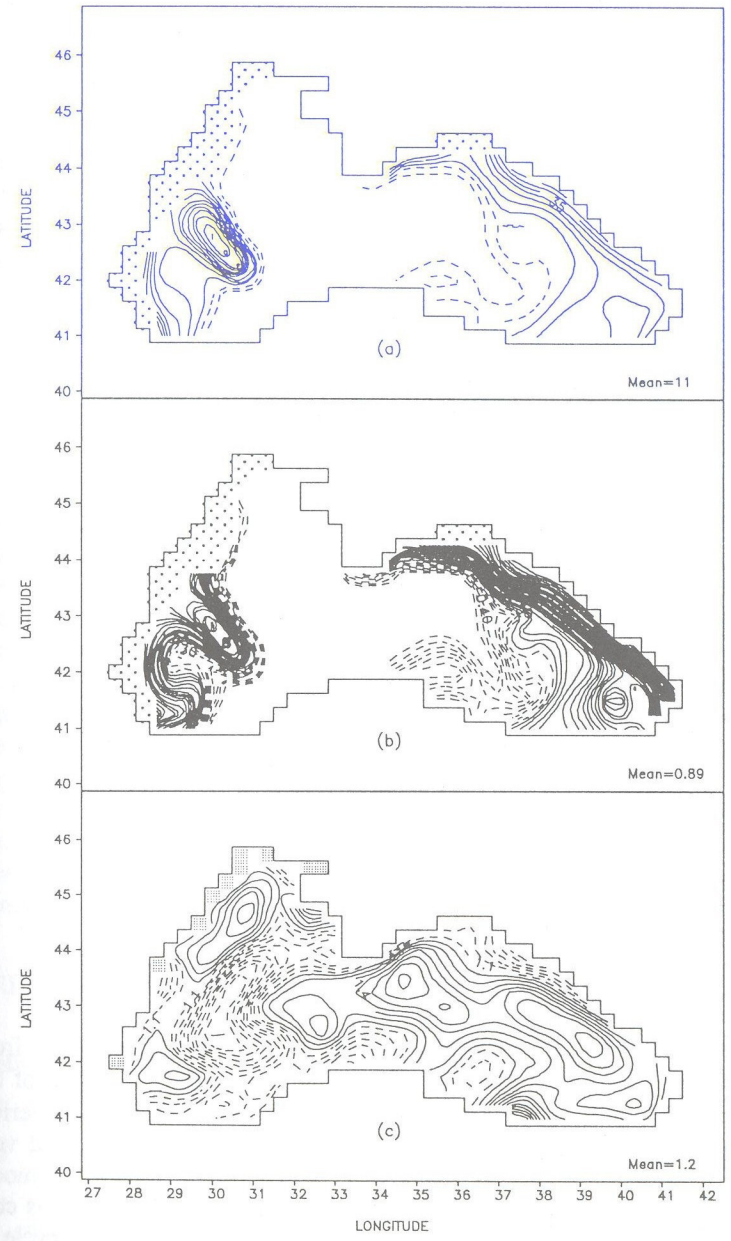


Figure 11. Snapshots of 3-D numerical model simulations at 19 March, 1982 for (a) depths of isopycnal surface  $\sigma_t=14.4$ , CI=5 m; (b) Nitrates concentrations at of isopycnal surface  $\sigma_t=14.4$ , CI=0.1 mmol N m<sup>-3</sup>; (c) Nitrates concentrations at depth 17.5 m, CI=0.1 mmol N m<sup>-3</sup>.

increase of the depth of pycnocline in the easternmost part of the sea and along the Caucasian coast is due to the general circulation. The nitrate concentration shows similar meandering patterns, particularly in the western Black Sea. The Batumi eddy is



clearly detected by the large values of nitrates caused by the increased entrainment from the deeper layers.

The horizontal patterns look quite different when plotted against depth. The simulations at 17.5 m show an upwelling of deep waters close to the surface in the eastern cyclonic gyres. This upwelling brings nutrient rich waters (Figure 11c) and allows more intense phytoplankton growth (Figure 12). In the western shelf the extreme convective events and the resulting mixing in the vertical supply the surface water with nutrient rich waters thus contributing to the increase of the phytoplankton biomass.

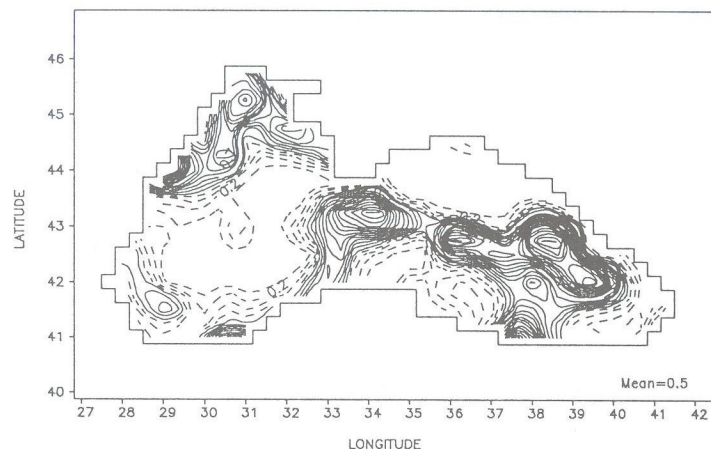


Figure 12. Concentration of phytoplankton at 19 March, 1982 at 2.5 m,  $CI=0.1 \text{ mmol N m}^{-3}$ .

## 5. Conclusions.

We use atmospheric forcing functions with time variability ranging from interannual to synoptic timescales to force a coupled physical/biological model of the Black Sea. One of our major tasks was to demonstrate the performance of numerical model for simulating the mixed layer evolution, as well as the response of a very simple biological system to variability in the physical conditions. The physical model reproduces quantitatively reasonably a number of features and processes, such as cold intermediate water formation, evolution of the seasonal thermocline, annual cycle of the MLD. Very important when using high frequency data is that the air-sea fluxes of heat and momentum depend on the model simulated SST, which tends to create important feedback mechanisms. Single events caused by the weather systems proved to be very important in the transfer of matter during the annual cycle. The transport of model nutrients across the halocline into the mixed layer is highly variable and mirrors

to larger extend the storm events. Thus, the entrainment from deeper layers enhances the interannual variability and causes the patchiness in phytoplankton patterns that is highly dependent on the physical model dynamics.

We showed that the seasonal cycle in the biological system is strongly controlled by the seasonal variability of mixed layer dynamics. About half of the variance in the primary production can be attributed to the spring weather conditions (Figure 7). It follows from the simulations that the interannual variability of the model biological system is mainly governed by the interannual variability in meteorological factors.

Horizontal advection and basinscale/mesoscale processes contribute substantially to the physical and biogeochemical variability in the ocean. This issue has been previously discussed by Doney (1996). However, most coupled physical-biological models are formulated only in the vertical coordinates, which tends to neglect the effects of advection. We have chosen to partially take these effects into account by analyzing simulation results obtained under different regimes of circulation, characterized by different vertical stratification. The comparison of vertical profiles of biogenic elements, simulated in the mixed layer model and in 3-D OGCM showed that the 1-D simulations carried out in different locations lie in the range of the basin wide variance of the 3-D simulations. However, this variance is rather large (comparable to the mean value) and the behavior of the model biological system in different Black Sea areas appears to be different. This suggests that 3-D modeling approach is necessary if the purpose is to produce reliable simulations of the ecological state of the Black Sea. The present study is only a preliminary work on this line and gives us a strong motivation for pursuing the three dimensional eddy-resolving modeling of physical and biogeochemical processes. The increase of horizontal resolution seems to be critical in the models to simulate very narrow biological fronts observed in the satellite data. Development of ecosystem model oriented to the specific Black Sea conditions and validation against observations is next major step toward increasing the consistency between models and observations.

**Acknowledgments:** This work is supported by the CEC Contract ERBIC15CT960113 to JVS and EVS

## References

- Berliand M. E., Berliand T. G. (1952). Measurement of the effective radiation of the Earth with varying cloud amounts. *Izv. Akad. Nauk, SSSR, Ser. Geofiz.*, 1, 64-78. (In Russian).
- Doney S. (1996). A synoptic atmospheric surface forcing data set and physical upper ocean model for the U.S. JGOFS Bermuda Atlantic time-series study site. *J. Geoph. Res.*, 101, C10, 25,615-25,634.
- Çokasar, T. (1997). Comparative analyses and seasonal modeling for the regional ecosystems of the Black Sea. M. Sc. Thesis. Middle east Technical University, Institute of Marine Sciences, 115 pp.
- Gill, A. and J. S. Turner (1976). A comparison of seasonal thermocline models with observations. *Deep. Sea Res.*, 21, 391-401.
- Goldman, C. R., A. Jasby and T. Powell (1990). Interannual fluctuations in primary production: Meteorological forcing at two subalpine lakes. *Limnology and Oceanography*, 34, 308-321.
- Gordon, C. and M. Bottomley (1985). The parameterization of the upper ocean mixed layer in Coupled ocean-atmosphere models. In: J.C.J. Nihoul (editor): *Coupled ocean-atmosphere models*. (Elsevier Oceanography Series, 40), Elsevier, Amsterdam, 613-637.



7. Gregoire M, J.-M. Beckers, J. Nihoul and E. Stanev (1997). Coupled hydrodynamic ecosystem model of the Black Sea at basin scale. E. Ozsoy and A. Mikaelyan (eds.): *Sensitivity to Change: Black Sea, Baltic Sea and North Sea*, NATO Series, Kluwer academic publisher, 487-499.
8. Fasham, M., H. Ducklow and S. McKelvie (1990). A nitrogen-based model of plankton dynamics in the oceanic mixed layer. *J. Mar. Res.*, **48**, 591-639.
9. Hellerman S., Rosenstein M. (1983). Normal monthly wind stress over the World Ocean with error estimates. *J. Phys. Oceanogr.*, **17**, 158-163.
10. Lowe P. R. (1977). An approximating polynomial for the computation of the saturation vapor pressure. *J. Appl. Met.*, **16**, 100 - 103.
11. Mikaelyan A. S. (1995). Winter bloom of the diatom *Nitzschia delicatula* in the open waters of the Black Sea. *Marine Ecology Progress Series*, **129**, 241-151.
12. Mitchell, J. F. B., C. Wilson and C. Price, 1985. On the specification of surface fluxes in coupled atmosphere-ocean general circulation models. In: J.C.J. Nihoul (editor): *Coupled ocean-atmosphere models*. (Elsevier Oceanography Series, 40), Elsevier, Amsterdam, 249-262.
13. Oguz, T., S. Besiktepe, O. Basturk, I. Salihoglu, D. G. Aubrey, et al. (1993). Cooperative Marine Science Program for the Black Sea (CoMSBlack' 92A). Physical and chemical intercalibration Workshop, Erdemli, Turkey, 15-29 January 1993. *IOC, Workshop Report No 98*.
14. Oguz T. and P. Malanotte-Rizzoli (1996). Seasonal variability of wind and thermohaline driven circulation in the Black Sea. *J. Geoph. Res.*, **101**, C7, 16551-16569.
15. Oguz, T. Ducklow P. Malanotte-Rizzoli, Turgul S., Nezhlin N. Unluata U. (1996). Simulation of annual plankton productivity cycle in the Black Sea by a one dimensional physical model. *J. Geoph. Res.*, **101**, C7, 16585-16599.
16. Ozsoy, E., U. Unluata and Z. Top (1993). The evolution of Mediterranean water in the Black Sea: interior mixing and material transport by double diffusive intrusions. *Progress in Oceanogr.*, **31**, 275-320.
17. Pakanowski, R. C., K. Dixon and A. Rosati (1991). The GFDL Modular Ocean Model Users Guide, version 1.0. GFDL Ocean Group Tech. Rep., No 2, 176 pp.
18. Paulson, C.A. and J. J. Simpson (1977). Irradiance measurements in upper ocean. *J. Phys. Oceanogr.*, **7**, 952-956.
19. Radach G. and A. Moll (1993). Estimation of the variability of production by simulating annual cycles of phytoplankton in the central North Sea. *Progr. Oceanogr.*, **31**, 339-419.
20. Rosati, A. and K Miyakoda (1988). A general circulation model for the upper ocean simulation. *J. Phys. Oceanogr.*, **18**, 1601-1626.
21. Sorkina A. I., Editor (1974). Reference book on the Black Sea climate. *Gidrometeoizdat*, Moscow, 406 pp.
22. Stanev, E. V. (1990). On the mechanisms of the Black sea circulation. *Earth-Science Rev.*, **28**, 285-319.
23. Stanev, E. V., J. V. Staneva and I. G. Gospodinov (1998). Numerical tracer model of surface and intermediate water formation in the Black Sea. (in this volume).
24. Stanev, E. V., J. V. Staneva, and V. M. Roussenov, (1997). On the Black Sea water mass formation. Model sensitivity study to atmospheric forcing and parameterization of some physical processes. *J. Mar. Sys.*, **13**, 245-272.
25. Staneva, J. V. and E. V. Stanev (1997). Cold water mass formation in the Black Sea and its sensitivity to horizontal resolution in numerical models. E. Ozsoy and A. Mikaelyan (eds.): *Sensitivity to Change: Black Sea, Baltic Sea and North Sea*, NATO Series, Kluwer academic publisher, 375-393.
26. Staneva J. V., Stanev E. V., Rachev N. H (1995). Heat balance estimates using atmospheric analysis data. A case study for the Black Sea. *J. Geophys. Res.*, **100**, C9, 18581-18596.
27. Staneva J. V., E. V. Stanev and V. M. Roussenov (1998). On the relative contribution of mixing and horizontal advection to the upper ocean dynamics. Intercomparison between 1-D and 3-D numerical model simulations. *J. Mar. Sys.* (submitted manuscript).
28. Van Eeckhout D. and Lancelot Ch. (1997). Modeling the functioning of the north-western Black Sea ecosystem from 1960 to present. E. Ozsoy and A. Mikaelyan (eds.): *Sensitivity to Change: Black Sea, Baltic Sea and North Sea*, NATO Series, Kluwer academic publisher, 455-468.
29. Wolf K. and J. Woods (1988). Lagrangian simulation of primary production in the physical environment - the deep chlorophyll maximum and nutricline. B. J. Rothschild (editor): *Towards a Theory of Biological-Physical Interactions in the World Ocean.*, Kluwer Academic Publishers, NATO ASI Series, 239, 51-70.

## COMPARATIVE ANALYSIS FOR REGIONAL ECOSYSTEMS

TÜLAY COŞKUN

Institute of Oceanography

P. O. Box 2

### Abstract.

A zero dimensional model is used to evaluate the behaviour of phytoplankton in the analyses of the seasonal cycle of chlorophyll-a in the model. In the coastal areas of the Black Sea, the model simulates the cent coastal area by riverine inputs. The concentrations generally follow the trend of data, it appears that in February-March in the peripheral regions, where a result of riverine and basic features of seasonal cycle. To interpret the available observed regional differences of the chlorophyll-a concentrations in the central Black Sea, it is found to be important along the coast. Downstream of the riverine input, the model results show a seasonal pattern of advection. Better representation of blooms are obtained with preliminary results are presented for the ctenophore *Mnemiopsis*.